JOURNAL OF Materials CHEMISTRY

Deposition of titania thin films from aqueous solution by a continuous flow technique

Tobias M. Fuchs,* Rudolf C. Hoffmann, Thomas P. Niesen,† Hannah Tew, Joachim Bill and Fritz Aldinger

Max-Planck-Institut für Metallforschung and Institut für Nichtmetallische Anorganische Materialien, Universität Stuttgart, Pulvermetallurgisches Laboratorium, Heisenbergstr. 3 D-70569 Stuttgart, Germany. E-mail: fuchs@aldix.mpi-stuttgart.mpg.de; Fax: 0049-711-6893-131; Tel: 0049-711-6893-103

Received 8th October 2001, Accepted 13th February 2002
First published as an Advance Article on the web 27th March 2002

Organic self assembled monolayer (SAMs) on *p*-type silicon (001) single crystal wafers were used as substrates for the formation of TiO_2 films from aqueous solution. It was previously shown that this organic modification allows the formation of homogeneous thin films of TiO_2 below 100 °C under static conditions. The formation of a titanium complex in the presence of H_2O_2 is used to avoid the otherwise spontaneous precipitation of titania from the aqueous solution. In the present paper, the synthesis of TiO_2 thin films is realized by a continuous flow method (cfm). In this method the silicon substrate is placed in a cylindrical reaction chamber, through which the solution is pumped with a constant flow rate. SEM, TEM, ellipsometry and XPS measurements illustrate that this technique allows deposition of thicker films than are obtained using a static deposition method, while achieving similar homogeneity. The films are crystalline and a uniform surface topography can be achieved.

Introduction

Thin films of titanium dioxide (TiO_2) have useful electrical and optical properties and excellent transmittance of visible light.

These properties make them suitable for applications such as dielectric layers in microelectronic devices,[1] high efficiency catalysts,[2] optical cells,[3] antifogging and self cleaning coatings,[4] gratings,[5,6] or gas sensors.[7] Conventionally, vapor phase deposition has been used to form high quality TiO_2 films. To coat complex-shaped substrates, sol–gel techniques with alkoxide precursors have been successfully applied.[8–11]

Recently there has been a growing interest for low-cost deposition techniques for ceramic thin films from aqueous solutions.[12] A promising technique is the use of templates such as organic self-assembled monolayers (SAMs) to induce and/or enhance deposition of oxides on a substrate.

SAMs are ordered molecular assemblies which are formed by chemical adsorption of a surfactant on the surface of a substrate. The functionalized surface is intended to promote the deposition of an inorganic phase, as proteins do in biomineralization. SAMs have shown convincing results on surfaces for promoting the formation of thin films of oxides such as SnO_2,[13,14] Fe_2O_3,[15] V_2O_5,[16] ZnO,[17] TiO_2[18–21] and ZrO_2[22–24] from aqueous solutions.

In previous work, deposition of titania thin films from aqueous solutions on SAMs was carried out.[18,19] To prevent spontaneous bulk precipitation, high concentrations of acid were used. Films usually were less than 100 nm thick and formed within 2–4 h. These films consisted of densely packed, randomly oriented TiO_2 crystals (usually anatase) with crystallite sizes of 2–4 nm. Koumoto *et al.*[25] deposited TiO_2 from hexafluorotitanate solution[26] using a patterned phenyltrichlorosilane SAM as substrate. Hydrophobic functionalities such as phenyltrichlorosilane are expected to suppress deposition of oxide films. In this case, areas where the SAM had been removed *via* Si–C bond photocleavage were coated by a film, while the deposits on the SAM could be removed by ultrasonication. Patterned titania films have also been formed after photolysis and oxidation of thioacetate-terminated SAMs through a mask, followed by immersion in the $TiCl_4$–HCl solution, which left the non-oxidized areas uncoated by titania.[27] High deposition rates were achieved by Baskaran *et al.*[20] using an aqueous titanium lactate solution to deposit titania films on plastic surfaces and SAMs. Recently, we reported[21] that TiO_2 films also form at low acidic concentrations in a static deposition process. Adherent films were formed on sulfonated SAMs from 10 mM TiO_2^{2+} solutions with an addition of 0.12 M HCl at 80 °C within 2 h. This addition of HCl was necessary to prevent visible bulk precipitation.

To reduce the deposition time and to achieve thicker films, continuous flow techniques have been used for films of SnO_2,[14] ZrO_2[24] or ZnO.[28] In these studies it was shown that pH and concentration of the solution play an important role in the growth mechanism of such films. In the present study, the growth behaviour of TiO_2 thin films in a continuous flow apparatus was investigated, using an inorganic titanium peroxide complex as developed previously.[21]

Experimental

Film deposition

p-Type {001} single-crystal Si wafers, approximately 10 × 10 mm^2 in size, were used as substrates. These wafers were polished, cleaned and oxidized in piranha solution (70 vol% of H_2SO_4, 30 vol% of 30 wt% H_2O_2 aqueous solution). Then the wafers were dipped into 1,1′-bicyclohexyl solution, containing 1 vol% of the surfactant (trichlorosilylhexadecane thioacetate) at room temperature under an inert atmosphere for several hours, during which the SAM formed spontaneously. Finally, the wafers were thoroughly washed in chloroform to remove all

†Present address: Siemens & Shell Solar GmbH, D-81739 München, Germany.

traces of surfactant. Further experimental details have been published elsewhere.[29,30]

The conversion of the thioacetate into the sulfonate ($-SO_3H$) group was realized by immersing the wafer in oxone (potassium hydrogenmonopersulfate, Merck) for a minimum of 4 h at room temperature.[30]

For continuous flow deposition a freshly prepared solution (10 mM TiO_2^{2+} and 0.12 M HCl; Ti concentration was verified by atomic absorption spectroscopy before use) was pumped (1.5 ml min^{-1}) through the reaction cell by use of a peristaltic pump for 1 h, 2 h, 4 h, and 6 h at 80 °C, providing constant concentrations of the reactants and preventing bulk precipitation in the reaction cell. The dimensions of the reaction cell are 2.5 cm in diameter and 7.5 cm in length. The SAM coated wafers were placed horizontally on a Teflon bar. This Teflon bar also reduces the size of the stagnant regions at both ends and improves the flow profile of the liquid in the cell. The solution over the substrate was kept *ca.* 5 mm deep, so that in the reaction cell there is a volume of *ca.*10 ml, analogous to ref. 14. Control experiments were done with piranha-oxidized Si wafers, *i.e.* without SAM.

Static deposition experiments were done for comparison. Here, the SAM coated substrates were immersed in 10 ml aliquots of the solution, covered, and then placed in an oil bath for the same reaction times and temperatures as in the continuous flow technique.

In both deposition methods, the samples where taken out of the solution after the determined reaction time and dried in flowing argon.

Film characterization

The resulting films were analysed using X-ray photoelectron spectroscopy (XPS) with a PHI 5400 ESCA. Microstructure analysis was done using a Zeiss DSM 982 Gemini field-emission scanning electron microscope (SEM) with an EDX attachment. The thickness of the films was measured using ellipsometry (Woollam M2000L with rotating compensator). For the fitting procedure, a refractive index of $n = 2.74$ for nanocrystalline TiO_2 particles was assumed after Kerr.[31] This fitting was based on a three-layer model with silicon as substrate ($n = 3.85$), an intermediate SiO_2–SAM layer (thickness 5 nm, $n = 1.45$) and the TiO_2 film on the top. The wavelength of the laser was 632.28 nm. The thickness was also determined by TEM images in cross-section (JEOL JEM 200 CX-TEM and JEOL JEM 2000 FX-TEM), which also provided microstructure analysis. The TEM was equipped with an EDX analyser with 200 kV energy. TEM sample preparation was done according to published procedures.[32] EDX and electron diffraction patterns were used for element and phase identification.

A Digital Instruments Nanoscope III AFM in non-contact mode was used for all AFM investigations. Scans were taken in air at room temperature.

Results

Experimental parameters were adapted from previous static depositions.[21] The flow rate of the solution in the reaction chamber was set to 1.5 ml min^{-1}. Lower flow rates led to bulk precipitation with little or no film formation. Higher flow rates led to less precipitation in the reaction cell, but also to less deposition on the sulfonated SAM, because the time the solution remains in the reaction cell was not long enough to initiate the deposition process.

The composition of the thin films was analysed by XPS. All peaks were calibrated using the C1s peak at 284.6 eV. After 1 h of deposition time, Ti signals at 464.7 eV (2p1) and 459.0 eV (2p3) were present, but also the small signal at 37.8 eV (Ti3p) and a peak for O1s at 530.8 eV. The Si signals at 154.6 eV (2s) and 103.6 eV (2p) were used to monitor the coverage of the substrate. The Si peaks vanished after 2 h deposition, demonstrating the full coverage of the SAM-modified substrate by the inorganic film.

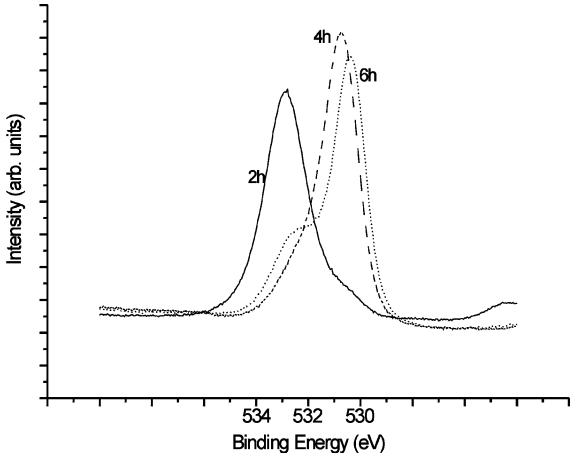

Fig. 1 XPS fits of the O1s peak for 2, 4 and 6 h samples.

In principle, XPS spectra should be able to reveal the presence of oxygen as hydrate, hydroxide or oxide.[33]

A curve fit for the oxygen signal (Fig. 1) shows that after 2 h of deposition the sample seems to contain water (533–534.5 eV) because of the shift of the peak to higher energies. The signal after 4 h is shifted to lower energies (532–530 eV), revealing the presence of OH. After 6 h the signal shows the lowest energies (528–532 eV), which can be attributed to oxide. This shift is characteristic for the formation of oxides from aqueous solutions.[34] Also a protrusion at the high energy side for the 6 h sample is visible, which indicates further crystallization, so that the oxygen signal can be attributed to titanium oxide and enclosed water only. Similar effects were reported for SnO_2.[14]

Ellipsometry measurements indicate an induction time of less than 1 h before film formation starts. After 1 h the average film thickness is 1 nm. Beyond 1 h deposition time, a high growth rate of about 70–100 nm h^{-1} is realized.

To compare the resulting film thickness under static and continuous flow condition, solutions from the same batch were used. Fig. 2 shows that with the continuous flow method, growth rate and thickness were enhanced drastically compared to that of the static deposition method. After 4 h deposition time, a decreasing growth rate is determined by ellipsometry which is a slight deviation from the results from cross-sectional TEM analysis described below.

Determined from the TEM micrograph, the film thickness after 2 h deposition time in continuous flow is 68 nm, which is in good agreement with the ellipsometry measurement (67 nm). The micrograph (Fig. 3) indicates a very homogenous film consisting of nanoparticles, and a layer consisting of the

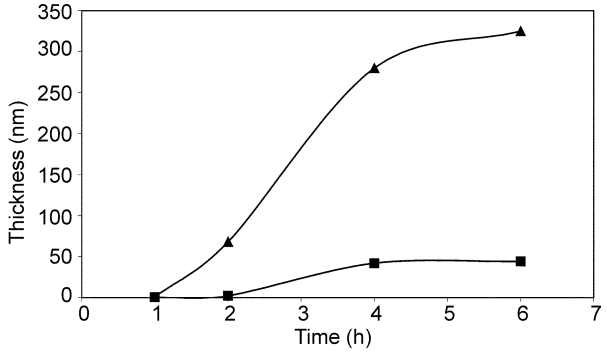

Fig. 2 Comparison of the achieved thickness by continuous flow (▲) and static deposition (■) methods (measured by ellipsometry).

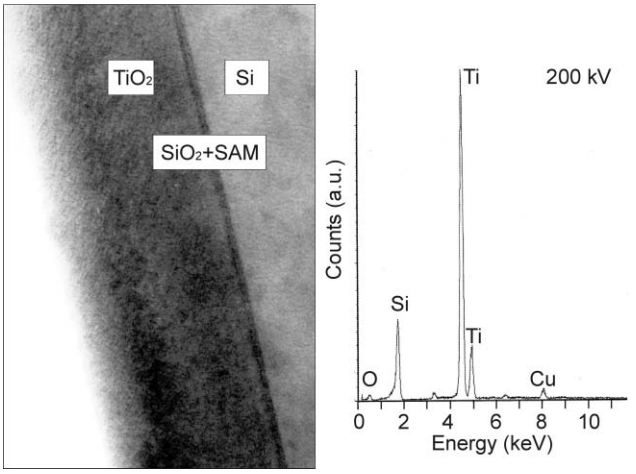

Fig. 3 TEM image after 2 h deposition and corresponding EDX spectrum.

oxidized Si surface and the SAM can be seen clearly (dark interlayer). The film is amorphous, as the electron diffraction pattern showed no spots of crystalline TiO_2 (not shown), although the EDX measurement (200 kV energy) shows the presence of strong Ti signals. (Cu signals in that image are an artefact resulting from sample preparation.)

The TEM cross-sectional image of a sample deposited over 6 h shows a nanocrystalline film. The diffraction pattern indicates that this film consists of anatase (Fig. 4). On the right side of that image, parts of the silicon substrate and the TiO_2 layer are missing as an artefact of the sample preparation. On the left side, the full thickness of the film and parts of the substrate are visible. The thickness of this film was determined to be 380–400 nm. In the film, grains up to 20–30 nm in size can be seen.

Fig. 5 shows that the film thicknesses determined by TEM and ellipsometry agree to within 5%. TEM analysis shows that the growth rate is approximately constant.

Further characterization was carried out by SEM and corresponding EDX measurements (Fig. 6). All EDX spectra were measured at the same energy of 10 kV. Therefore, the presence and intensity of the Si signal is a rough probe for the film thickness.

In samples obtained after a deposition time of 1 h, SEM micrographs indicate the presence of particles. However, the corresponding EDX measurement did not indicate any Ti signals but high amounts of O. The particles do not cover all the substrate and have a height of 10–15 nm. After 4 h deposition time, the film was almost continuous and the EDX

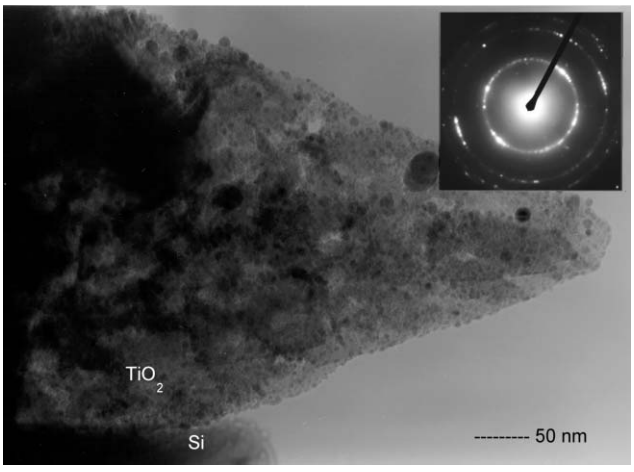

Fig. 4 TEM image after 6 h deposition and corresponding electron diffraction pattern.

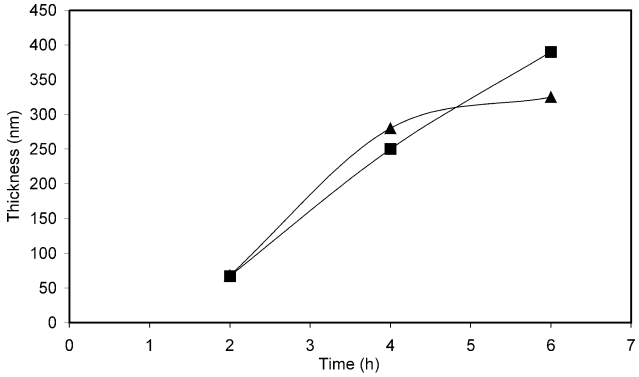

Fig. 5 Comparison of the determined ellipsometry (▲) and TEM (■) thickness (nm).

spectra reveal clear Ti peaks. After 6 h deposition time, a continuous film can be seen and the corresponding EDX measurement indicates the film to be TiO_2. The absence of the Si signal gives an estimation of the film thickness of 300 nm after 6 h reaction time after.[35] Also some bigger particles can be seen at the surface, in agreement with the 6 h TEM image (Fig. 4).

AFM investigations of these samples show surface inhomogenities which are 20 nm in size after 1 h deposition (Fig. 7) and increase with longer reaction time. These results are in good agreement with those estimated by SEM analysis (10–15 nm).

After 6 h deposition, the RMS roughness is about 12 nm and the maximum roughness is 132 nm.

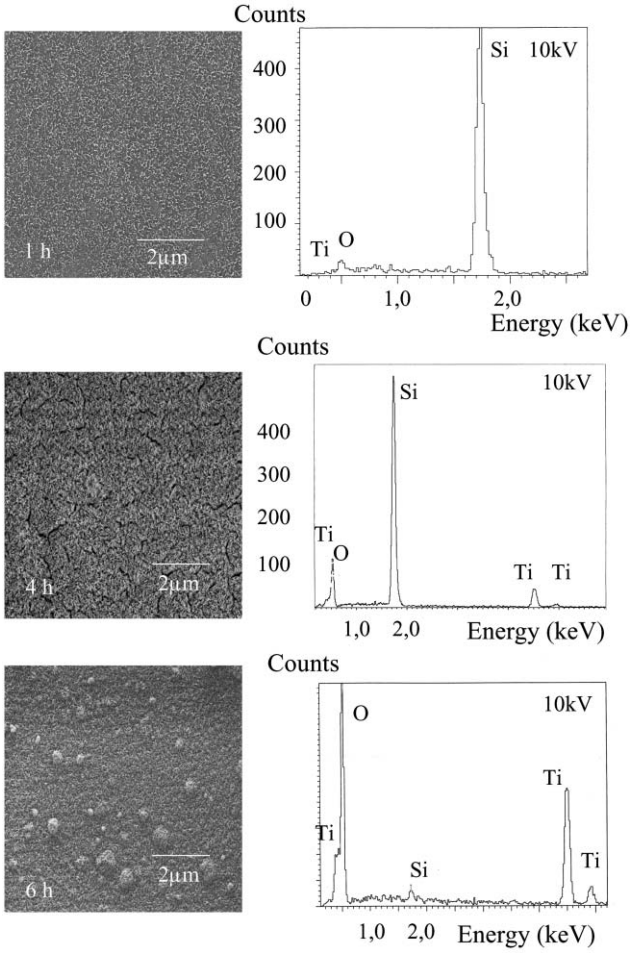

Fig. 6 SEM images and corresponding EDX spectra after 1, 4 and 6 h deposition.

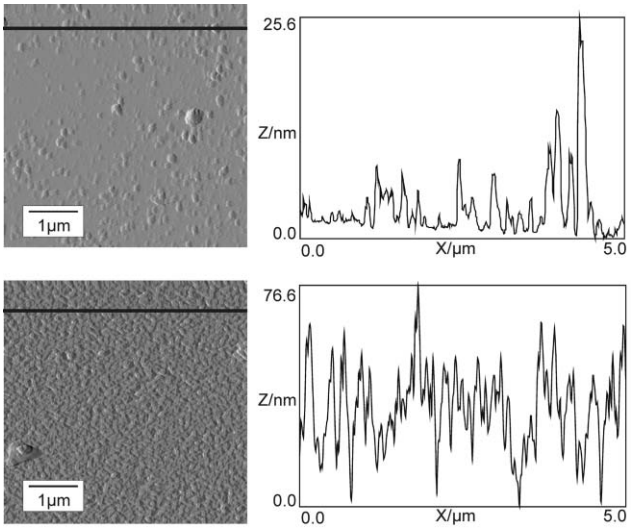

Fig. 7 AFM images and corresponding roughness spectra after 2 (upper) and 6 h (lower) deposition time.

Discussion

The deposition rate and thickness of the films can be increased substantially by applying the continuous flow technique.

The linear growth rate determined by TEM analysis (Fig. 5) shows that the cfm achieves constant growth conditions by continuously replenishing the deposition solution. In contrast, the stagnation of growth in the static deposition method at longer deposition times can be attributed to a decrease in the concentration of reactants in the solution.

The decreasing growth rate at longer deposition times in the ellipsometry measurements (Fig. 5), may be an artefact caused by the fitting parameters used, which are in less good agreement for thicker films (see film characterization). Another possibility for the lower growth rate in this measurement technique is the formation of an inhomogeneous film topography of thicker films as seen in former TEM and AFM investigations.[21]

AFM investigations show an increase of surface inhomogeneities after 6 h deposition time (Fig. 7) compared to the sample deposited in 1 h. TEM investigation of the sample deposited over 6 h (Fig. 4), which gives a film thickness of 380–400 nm, indicates that surface inhomogeneities seem to be the most probable reason for the overall decrease of the growth rate determined by ellipsometry. The surface topography also may be affected by grain growth, because after 2 h deposition time a homogenous film is realized and after 6 h crystals in the nanometer scale (3–30 nm) within the film can be seen clearly.

From AFM measurements, the thickness-to-roughness ratio achieved under continuous flow of the solution was about the same as in films from static depositions.[21] Also the RMS roughness is similar (about 12 nm).

In the TEM image of the sample after 2 h deposition time, darker and brighter regions in the film can be seen. The dark areas may correspond to denser packed areas consisting of smaller nanoparticles (*ca.* 5 nm). The white features between the grains correspond most probably to an amorphous hydrous titanium oxide, formed by bulk precipitation of the solution and trapped between these grains during air-drying. The nanocrystalline nature of the film is the reason for the rings in the diffraction pattern (not shown here).With increasing deposition time, crystallization and grain growth in the film occurs, so that distinct spots can be seen in the diffraction pattern after 6 h reaction time. This assumption is supported by the XPS measurements, which indicate a decrease in the crystal water content of the film. Therefore, it is suggested that amorphous titanium hydroxide species tend to dehydrate with longer reaction times and form nanocrystalline titanium oxide type species.

In the SEM images, it can be seen that film growth starts with the growth of particles (islands?) on the substrate (1 h). With longer reaction time more and more particles are formed out of the solution which then grow together and form the film. This is also a possible indication of the increase of inhomogenities in the formed films.

The comparison of the formation of TiO_2 and SnO_2 thin films[36] by a continuous flow technique shows that there is in both cases an optimum flow rate of the precursor solution for a maximum growth rate of the film (TiO_2 *ca.* 70 nm h^{-1}, SnO_2 *ca.* 10 nm h^{-1}). In contrast to TiO_2, SnO_2 also forms on bare silicon substrates but needs a longer incubation time (1.5 h) in this case. The XPS results (oxygen fit) indicate similar formation behaviour for TiO_2 and SnO_2. The formation of amorphous material at the beginning of deposition contrasts with the SnO_2 films, which were nanocrystalline at all stages of growth. In further contrast to the SnO_2 films, for which the crystal size was constant at 4–10 nm for deposition times up to 15 h, the TiO_2 crystals reported here increased in size with deposition time. The formed TiO_2 films had the highest thickness achieved by this technique so far within 6 h in comparison to SnO_2 or ZrO_2.

That the films from the continuous flow technique have higher thickness and show smaller particle size may be the result of colloidal particles that form in the solution. The attraction to the substrate would then be the result of a net attraction resulting from the summation of electrostatic, van der Waals, and hydration interactions. When the size of the particles exceeds a certain value, these forces will be negligibly small.[21] Therefore only small particles can adhere to the film. In the continuous flow apparatus, fresh solution is always available and therefore only nanoparticles are present to attach to the substrate. In contrast, during deposition in a static medium, the starting nanoparticles increase in size and the metal ion concentration of the solution decreases. Lastly, we note that no TiO_2 films formed on bare silicon, but only on SAM-modified surfaces, whether from a static or a flowing medium.

Conclusions

A new way to deposit nanocrystalline thicker titania films from aqueous solution on modified silicon {001} single crystal wafers is reported. The results demonstrate the benefit of constant conditions like concentration, flow rate and temperature of the solution during deposition in a continuous flow apparatus. So the growth rate, film thickness and crystallinity of the films can be inproved. An intereseting point is, that the films formed on SO_3H–SAMs but not on bare silicon {001} wafers.

There may be potential for further improvements in the achievement of thicker, even more crystalline films with a finer microstructure by investigating the optimization of the reaction time, solution temperature and the concentration of the chemicals. Also an optimization of the flow rate is perhaps possible.

Acknowledgement

The authors thank H. Labitzke, M. Kelsch, A. Zern and P. Graat, for providing support with characterization of the films and Wacker Silitronic AG for supplying the silicon wafers. Helpful discussions with Prof. M.R. DeGuire (CWRU, Cleveland, OH) are gratefully acknowledged. This work was financially supported by the Deutsche Forschungsgemeinschaft (Al 384/22-3).

References

1 G. P. Burns, *J. Appl. Phys.*, 1989, **65**, 2095–2097.
2 T. Carlson and G. L. Griffin, *J. Phys. Chem.*, 1980, **84**, 5896–5900.
3 B. E. Yoldas and T. W. O'Keeffe, *Appl. Opt.*, 1979, **18**, 3133–3138.
4 R. Wang, K. Hashimoto and A. Fujishima, *Nature*, 1997, **388**, 431–432.
5 S. I. Borenstain, U. Arad, I. Lyubina, A. Segal and Y. Warschawer, *Thin Solid Films*, 1999, **75**, 2659–2661.
6 J. A. Quintana, P. G. Boj, J. Crespo, J. A. V. Abarca and J. M. Villalvilla, *Thin Solid Films*, 1998, **317**, 343–346.
7 M. Nabavi, S. Doeuff, C. Sanchez and J. Livage, *Mater. Sci. Eng. B*, 1989, **3**, 203–307.
8 C. J. Brinker and G. W. Scherer, *Sol–Gel Science: The Physics and Chemistry of Sol–Gel Processing*, Academic Press, San Diego, CA, 1990.
9 H. L. M. Chang, J. C. Parker, H. You, J. J. Xu and D. J. Lam, *Mater. Res. Soc. Symp. Proc.*, 1990, 168.
10 E. T. Fitzgibbons, K. J. Sladek and W. H. Hartwig, *J. Electroceram. Soc.*, 1972, **119**, 735.
11 L. M. Williams and D. W. Hess, *J. Vac. Sci. Technol., A*, 1983, **A1**, 1188–1192.
12 T. P. Niesen and M. R. DeGuire, *J Electroceram.*, 2001, **6**, 169–207.
13 B. Bunker, P. Rieke, B. Tarasevich, A. Campbell, G. Fryxell, G. Graff, L. Song, J. Liu, J. Virden and G. McVay, *Science*, 1994, **264**, 48–55.
14 S. Supothina and M. R. DeGuire, *Thin Solid Films*, 2000, **371**, 1–9.
15 M. Matai, M.S. Thesis, Case Western Reserve University, Cleveland, OH, 1994.
16 T. P. Niesen, J. Wolff, J. Bill, M. R. DeGuire and F. Aldinger, *Mater. Res. Soc. Symp. Proc.*, 1999, **576**, 197–202.
17 M. R. DeGuire, T. P. Niesen, S. Supothina, J. Wolff, J. Bill, C. N. Sukenik, F. Aldinger, A. H. Heuer and M. Rühle, *Z. Metallkd.*, 1998, **89**, 758–766.
18 H. Shin, R. J. Collins, M. R. DeGuire, A. H. Heuer and C. N. Sukenik, *J. Mater. Res.*, 1995, **10**, 692–698.
19 H. Shin, R. J. Collins, M. R. DeGuire, A. H. Heuer and C. N. Sukenik, *J. Mater. Res.*, 1995, **10**, 699–702.
20 S. Baskaran, L. Song, J. Liu, Y. L. Chen and G. L. Graff, *J. Am. Ceram. Soc.*, 1998, **81**, 401–408.
21 T. P. Niesen, J. Bill and F. Aldinger, *Chem. Mater.*, 2001, **5**, 1552–1559.
22 M. Agarwal, M. R. De Guire and A. H. Heuer, *J. Am. Ceram. Soc.*, 1997, **80**, 2967–2981.
23 A. Fischer, F. C. Jentoft, G. Weinberg, R. Schlögl, T. P. Niesen, J. Bill, F. Aldinger, M. R. DeGuire and M. Rühle, *J. Mater. Res.*, 1999, **14**, 3725–3733.
24 T. P. Niesen, T. Fuchs, J. Bill, F. Aldinger, U. Sampathkumaran and M. DeGuire, *Materials Week 2000—Proceedings*, Werkstoff-woche-Partnerschaft, Frankfurt, 25–28 September 2000, url: www.materialsweek.org/proceedings
25 K. Koumoto, S. Seo, T. Sugiyama and W. S. Seo, *Chem. Mater.*, 1999, **11**, 2305–2309.
26 S. Deki, Y. Aoi, O. Hiroi and A. Kajinami, *Chem. Lett.*, 1996, 433–434.
27 R. J. Collins, H. Shin, M. R. DeGuire, A. H. Heuer and C. N. Sukenik, *Appl. Phys. Lett.*, 1996, **69**, 860–862.
28 K. Ito and K. Nakamura, *Thin Solid Films*, 1996, **286**, 35–36.
29 N. Balachander and N. Sukenik, *Langmuir*, 1990, **6**, 1621–1627.
30 R. Collins and C. Sukenik, *Langmuir*, 1995, **11**, 2322–2324.
31 P. F. Kerr, *Optical Mineralogy*, McGraw-Hill, New York, 1977, pp. 72–80.
32 A. Strecker, U. Salzberger and U. Mayer, *J. Prakt. Metallogr.*, 1993, **30**, 428.
33 C. L. Lau and G. K. Wertheim, *J. Vac. Sci. Technol.*, 1978, **15**, 622–624.
34 C. D. Wagner, W. M. Riggs, L. E. Davis, J. F. Moulder and G. E. E. Muilenberg, *Handbook for Photoelectron Spectroscopy*, PerkinElmer Corporation, Eden Prairie, MN, 1978.
35 P. F. Schmidt, *Praxis der Rasterelektronenmikroskopie und Mikroanalyse*, Expert Verlag, Renningen-Malmsheim, Germany, 1994.
36 S. Supothina, Ph.D. Thesis, Case Western Reserve University, Cleveland, OH, 1999.